Optical limiting and non linear optical properties of fullerene derivatives embedded in hybrid sol–gel glasses

ARTICLE *in* CARBON · JANUARY 2000

Impact Factor: 6.2 · DOI: 10.1016/S0008-6223(00)00055-5

9 AUTHORS, INCLUDING:

Renato Bozio
University of Padova
169 PUBLICATIONS **3,174** CITATIONS
SEE PROFILE

Plinio Innocenzi
Università degli Studi di Sassari
211 PUBLICATIONS **4,818** CITATIONS
SEE PROFILE

Massimo Guglielmi
University of Padova
238 PUBLICATIONS **4,100** CITATIONS
SEE PROFILE

PERGAMON

Carbon 38 (2000) 1653–1662

CARBON

Optical limiting and non linear optical properties of fullerene derivatives embedded in hybrid sol–gel glasses

Raffaella Signorini[a,*], Moreno Meneghetti[a], Renato Bozio[a], Michele Maggini[b], Gianfranco Scorrano[b], Maurizio Prato[c], Giovanna Brusatin[d], Plinio Innocenzi[d], Massimo Guglielmi[d]

[a]*Dipartimento di Chimica Fisica, Università di Padova, Via Loredan 2, I-35131 Padova, Italy*
[b]*Centro Meccanismi di Reazioni Organiche del CNR, Dipartimento di Chimica Organica, Università di Padova, Padova, Italy*
[c]*Dipartimento di Scienze Farmaceutiche, Università di Trieste, Trieste, Italy*
[d]*Dipartimento di Ingegneria Meccanica, Università di Padova, Padova, Italy*

Abstract

Non linear optical properties of pyrrolidino-fullerenes in sol–gel matrix have been investigated for Optical Limiting (OL) applications. The fullerene functionalization increases the solubility in polar solvent and allows the preparation of solid materials via sol–gel method. It also extends the absorption of fullerenes to the red spectral region, where the maximum of the triplet to triplet absorption spectrum is located and, as a result, the Reverese Saturable Absorption (RSA) mechanism is enhanced. The use of the sol–gel method allows the preparation of samples with controlled thickness, with very good linear and non linear optical properties and with high damage fluences. This is useful to design and prepare a bottleneck structure, in order to optimize a laser protection device. The test of the non-linear optical properties of sol–gel samples containing fullerene derivatives has been made by optical limiting and Z-scan measurements and by comparing the experimental data with the calculated RSA behavior. Fullerene derivatives show good optical limiting performances in the red spectral region, better than fullerene. The pyrrolidino-fullerenes in sol–gel samples still show the same performances as solution samples. The comparison of the experimental data with the theoretical OL curves indicates that RSA is the predominant OL behavior, especially at 690 nm, but other different mechanisms, like non linear scattering, may contribute and are being considered in refining our theoretical model. The control of the propagation beam geometry is one of the critical point for OL measurements as well as for the optimal design of a protecting device.

Keywords: A. Fullerene; C. Modeling; D. Optical properties

1. Introduction

A common problem in the laser technology is the protection of optical sensors and of the human eye from the damaging effects of high-energy laser light. A solution to this problem is the use of passive optical limiters as protection devices. A material possesses optical limiting (OL) properties when its optical absorption increases as the incident beam intensity increases in such a way that the transmitted intensity never exceeds a damage threshold level. It is further required that the linear transmittance is high enough not to limit the detector response at ordinary signal levels. This can be achieved by different non-linear (NL) optical mechanisms [1]: coherent NL absorption (two or three photon absorption), NL scattering, thermal lensing, etc. Among NL absorption processes, reverse saturable absorption (RSA) is one of the best processes to use for OL because it reduces the total pulse energy rather than simply reducing the fluence or irradiance.

RSA arises generally in a molecular system when the excited state absorption cross section is larger then the ground state cross section at the input laser wavelength. To understand the process we can consider the electronic energy levels represented in Fig. 1, where the σ_i^n symbols designate the absorption cross section (of singlet and triplet states) and τ_i their lifetimes.

*Corresponding author. Tel.: +39-4-9827-5130; fax: +39-4-9827-5135.

E-mail address: raffy@chfi.unipd.it (R. Signorini).

0008-6223/00/$ – see front matter
PII: S0008-6223(00)00055-5

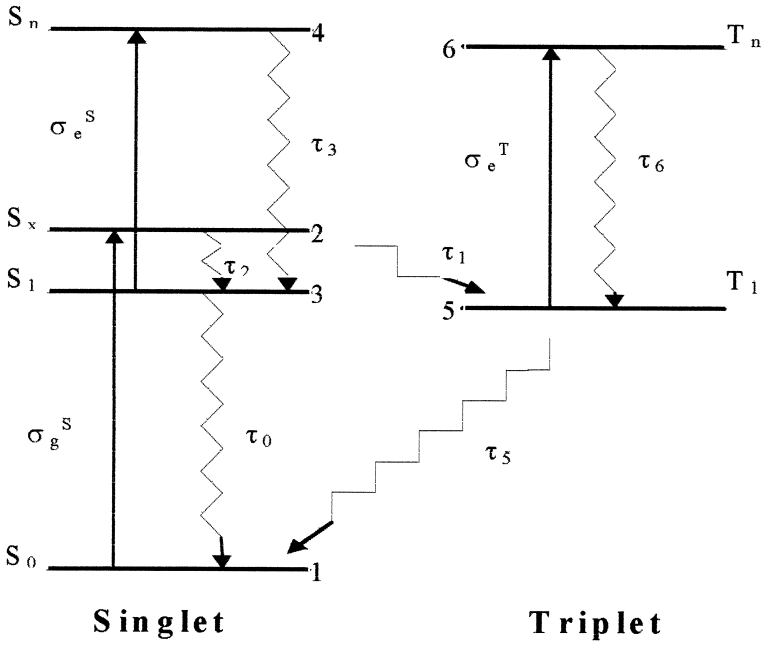

Fig. 1. The electronic energy levels of singlet (S_i) and triplet (T_i) states of fullerenes are illustrated. Absorptions are correlated to the absorption cross sections of the states (σ_i), the emission to the relaxation time (τ_i). S_0 represents the ground state, S_1 and T_1, respectively, the first singlet and triplet excited states, S_x a vibrational state of S_1, S_n and T_n higher singlet and triplet excited states.

As the material absorbs light, the first excited (singlet) state becomes populated and, in its turn, contributes to the total absorption of the material. If $\sigma_e^S < \sigma_g^S$, the material becomes more transparent (i.e. it is a saturable absorber), if $\sigma_e^S > \sigma_g^S$, the total absorption increases: the material is then a reverse saturable absorber. A three-level scheme is commonly used to describe RSA when sub-nanosecond time pulses are used. For longer pulses, significant inter-system-crossing (ISC, Φ) to a triplet state occurs in some systems. In these cases the excited state absorption occurs from the lowest triplet to higher excited triplet states.

Under appropriate conditions, the population accumulates in the lowest triplet state during the pulse and it provides an increasing contribution to the total absorption of the system. The significant parameters for the effectiveness of this mechanism are the excited state lifetimes and the ISC time, compared with the duration of the laser pulse, and the values of the absorption cross sections. In a more general RSA mechanism, the strongly absorbing electronic excited states can be populated by other incoherent processes as well (e.g., internal conversion, energy transfer).

Owing to their high molecular symmetry, fullerenes exhibit a weak ground-state absorption in most of the visible range that is attributed to symmetry-forbidden transitions, weakly allowed by vibronic coupling. In the same region, both the singlet and triplet excited-state absorptions are much stronger, with the triplet–triplet absorption peaking at 750 nm in C_{60} [2]. Fullerene is characterized by a very high value of the quantum yield for ISC: the triplet state is populated from the lowest singlet state in the nanosecond time scale. These features make C_{60} a favorable NL absorber (via RSA) in a large range of the visible spectrum, thus a good candidate for optical limiters for protection against frequency agile laser sources.

The increasing interest in fullerene (C_{60}) and its derivatives is due to their chemical and optical properties. However, C_{60} itself is hardly processible into a solid optical material, like doped polymers (e.g. PMMA [3]) and sol–gel glasses, owing to its very low solubility in solvents commonly used for their preparation. For this reason much work has been done to synthesize new derivatives with higher solubility maintaining the same NL optical properties. We have recently shown that appropriate fullerene functionalization increases the solubility in polar solvent and allows the preparation of solid materials via sol–gel method [4]. The presence in the fullerene derivatives of reactive groups that can covalently bind the inorganic network allows the optimization of the sol–gel procedures and the preparation of transparent films and bulk samples with good optical performances. At the same time, since the high fullerene symmetry is broken, a new transition around 690 nm becomes allowed and fullerene derivatives absorb at longer wavelengths where C_{60} is practically transparent [5]. As a result, transferring population from the ground to the excited triplet state by optically pumping in the red and deep-red region is much easier with the

fullerene derivatives than with C_{60}. Furthermore, the lowest triplet state absorption that peaks around 750 nm in C_{60} shifts to about 700 nm in the fullerene mono-adduct derivatives. The improved overlap of ground state and triplet absorption, while maintaining $\sigma_T > \sigma_G$, is obviously beneficial for the RSA mechanism [6–8].

In this paper we compare the OL behavior of a pirrolydino-fullerene derivative (hereafter FULP) solution with a FULP doped sol–gel sample and we show that the inclusion in the sol–gel matrix does not affect the OL performances of the fullerene derivative. The OL experimental data are compared with calculated curves based on an RSA model in order to evaluate the RSA contribution to the OL of the materials. The contribution of NL scattering effects has also been investigated by comparing open aperture and closed aperture OL measurements of solutions and of solid materials. The OL performances of multilayer structures, prepared according to Miles' prescriptions [9] for bottleneck optical limiters, have been compared with theoretical calculation in order to estimate the applicability of the model and its limits and evaluate the prospects for practical protection devices.

2. Experimental

The fullerene functionalization is a well known process [10,11]. The thermal ring-opening of aziridines with electron-withdrawing substituents in the presence of C_{60} generates the pyrrolidino-fullerene (FULP) [12], shown in Fig. 2. The monoaddition product can be isolated with good yields. FULP has high solubility (43 mg ml^{-1}) [12] in THF.

Our attention has been focused on 3-(glycidoxypropyl)-trimethoxysilane (GPTMS) [13] based hybrid sol–gel glasses as host materials. GPTMS is an organically modified alkoxide containing an epoxide ring in the organic functional groups. By opening and cross-linking of the epoxy a polyethylene oxide chain is formed interpenetrating the inorganic silicon oxide network.

GPTMS derived sol–gel coatings have shown [13] good anti-scratch resistance, low optical absorption in the visible range and good thermal stability, very thick coatings are, also, easily fabricated. These properties make materials based on GPTMS good candidates for high OL performances.

A key point in the synthesis of GPTMS materials is the choice of the epoxy ring opening catalyst. It must be considered that this catalyst can also be a network former, such as the commonly used titanium and zirconium alkoxides, which modifies the material properties and moreover needs the use of chelating agents to control the sol–gel reaction. The choice of other catalysts, must be carefully evaluated, because strong acids or bases can catalyse the hydrolysis and condensation reactions also of the inorganic side. A too fast formation of one of the two chains, the inorganic or the organic, can hinder the

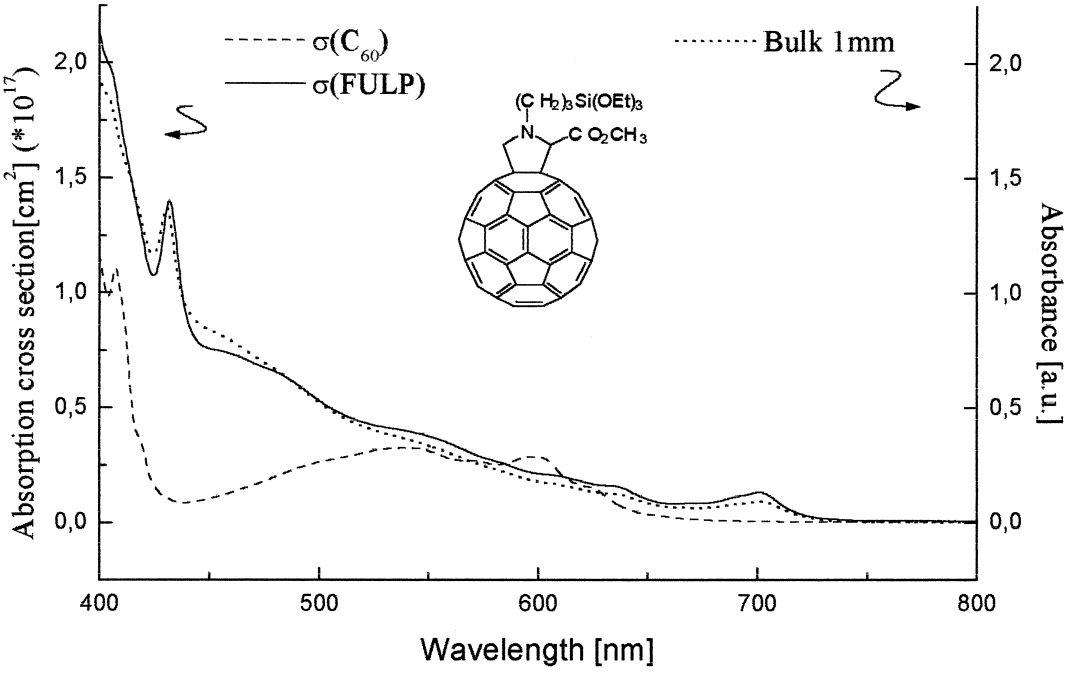

Fig. 2. Linear absorption spectra of FULP (solid line) and C_{60} (dashed line) solutions in toluene, 10 mm thick, and of a FULP doped sol–gel sample (dotted line), 1 mm thick.

polymerisation of the other one, changing the microstructural properties of the matrix in an undesired way.

The useful sol–gel matrix is called: *3-(glycidoxypropyl)-trimethoxysilanetetraethoxysilanezirconium butoxide (GTZ).* The sol was prepared by using zirconium butoxide ($Zr(OBut)_4$) to catalyse the organic polymerisation by opening the epoxy ring. $Zr(OBut)_4$ was added to GT together with 2,4-pentanedione (acac) as chelating agent. The molar ratios were $Zr(OBut)_4$: (GPTMS + TEOS) = 0.1 $Zr(OBut)_4$: acac = 0.5. After the addition of $Zr(OBut)_4$ the sol was refluxed 1 h at 80°C and then used for the materials processing. In order to dope the matrix, FULP was dissolved in tetrahydrofuran and then this solution was added to the precursor sols.

To determine the exact molar concentration of fullerene in the solid matrices a procedure has been developed to convert the molar ratio C_{60}/MO_2 (M = Si and/or Ti and/or B) to C_{60} molarity. The first value is known by adding a controlled amount of C_{60} to a sol, in which the molar concentration of alkoxide is controlled. When the glass is obtained, the density of the material (g/cm^3) is measurable but it is not convertible to the density mol/cm^3. In fact, the stoichiometry of the molecule is not known because OH and organic residual groups are present. For this reason treating the material at 1200°C, only the oxide MO_2 remains and it is directly correlated to the initial alkoxide content. Taking into account the weight loss, the density of MO_2 expressed in MO_2/cm^3 is calculated. This value permits to convert the molar ratio C_{60}/MO_2 into C_{60} molar concentration.

Coating films were obtained from fresh sols by dip-coating or spin-coating. The samples were typically thermally treated in air at 120°C for 1 h. The film thickness was measured by a profilometer (Alpha Step 200, Tencor Instrument). Bulk samples were prepared putting the precursor sols in a PP box at 60°C for 24 h.

Multilayer structures of 3–10 layers were prepared by evaporating the solvent from the sol depositing the viscous solution between sodalime slides of appropriate thickness. The thickness of the sol–gel doped layers is controlled by appropriate spacers.

The density of the bulk samples was measured by a picnometer in water.

Optical limiting measurements were performed using an excimer pumped pulsed dye laser (Lambda Physik FL2002) operating with different dyes (Coumarine 503 and LDS 690) and emitting 10 ns pulses at either 532 nm or 690 nm, with 1 Hz repetition rate. The laser beam was focused onto the sample using a 200 mm achromatic lens. The incident and transmitted laser pulse energies were measured by using either photodiodes calibrated against the signal from a surface absorbing calorimeter or a pyroelectric detector.

The Z-scan method [14] is a simple technique to determine the NL changes of refractive index and absorption. The transmission of the sample is monitored, by using a photodiode through an aperture, while varying the sample position (along the longitudinal Z-axis) in the vicinity of the focal position of a fast focusing optical system. An iris in front of the detector can be set with a narrow or a wide aperture (for closed or open aperture Z-scan measurements, respectively). In the first case, only the laser beam passes through the aperture so that the signal intensity is affected both by the NL absorption and by the NL refraction. In the latter case, it is possible to investigate the effect of the NL absorption alone. By comparing open and close aperture Z-scan data it is possible to single-out the NL changes of refractive index. On the other hand, open aperture Z-scan measurements make it possible to locate the position of maximum absorption even in the presence of NL refraction effects (e.g., thermal lensing).

3. Results and discussion

The linear optical properties of FULP are reported in Fig. 2, where the visible and near-infrared absorption spectrum of FULP is shown and compared with that of fullerene. C_{60} shows a weak absorption between 450 and 650 nm. In the same region, beside a narrow peak at 430 nm, FULP shows a similar broad absorption which continues as far as 700 nm. Both the narrow peak and the additional deep-red absorption are typical of other 1,2-dihydrofullerens. [6–8] As recalled above, the triplet to triplet absorption of FULP peaks at about 700 nm compared to 750 nm for C_{60}. This makes possible to conclude that in the red region the RSA mechanism of fullerenes should be enhanced compared to the green region and this is expected to an ever greater extent for FULP [2,3,6–8]. This fact has been verified by comparing OL measurement of FULP and C_{60} at 532 nm and at 690 nm [12]. By comparing C_{60} and FULP, one concludes that they have very similar behavior, but the efficiency of the FULP in the red spectral region is remarkably better. The very low absorption of C_{60} at 690 nm implies that the transfer of population to the triplet state requires, in this case, high input fluences, much higher than for FULP. This fact and the peaking of the triplet absorption of FULP at 700 nm determines the differences of its behavior with respect to C_{60}.

Fig. 2 also reports the linear absorption spectrum of a 1 mm sol–gel matrix doped with FULP. By comparing the solution and the sol–gel absorption spectra one observes that the inclusion of FULP in the sol–gel matrix does not affect the linear properties of fullerene derivatives. Furthermore, the optical quality of our matrix is very good and it allows the inclusion of high concentration of FULP without the problem of its aggregation [15,16], a situation which should be avoided since aggregation produces a degradation of the OL behavior.

In order to verify whether the NL optical properties of

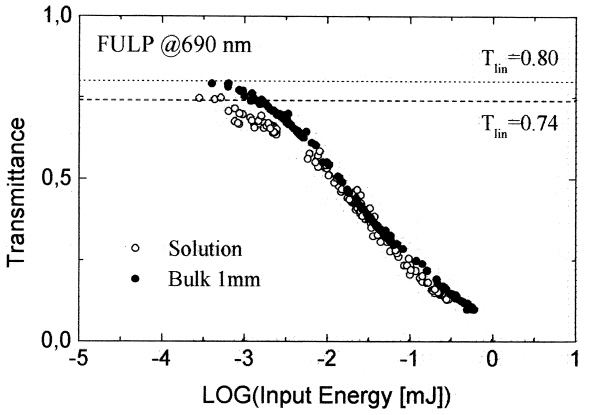

Fig. 3. OL data: transmittance vs. input energy at 690 nm of FULP toluene solution, with linear transmittance 0.74, and 1 mm FULP doped bulk sol–gel sample, with linear transmittance 0.80.

FULP in solid samples do not differ appreciably from those in solution, we compared OL measurements of a FULP solutions with those of a sol–gel sample having similar thickness and linear transmittance. For this purpose, a sample has been prepared consisting of 1 mm FULP doped sol–gel bulk, with linear transmittance T_{lin} = 0.80.

Our OL experimental data are reported as transmittance as a function of input energy. It is not very informative to report the data as a function of input fluence since the beam-waist size is changing during the OL measurement due to thermal lensing which occurs in our samples as the energy increases (see below).

Fig. 3 reports OL data of a 10 mm FULP solution in toluene, with linear transmittance T_{lin} = 0.74, and of the bulk sample at 690 nm. The experimental data show that in the sol–gel matrix we obtained an OL performance very similar to that of solution samples. This shows that it is possible to include fullerene derivatives in solid matrix without affecting the good NL properties of the molecules in solution.

A summary of our results in the characterization of the OL properties of C_{60} and FULP solutions is given in Table 1. Table 2 provides the corresponding data for FULP in sol–gel samples.

The data in Table 1 demonstrate the enhanced OL efficiency in the red spectral region (690 nm) compared to the green one (532 nm) for both C_{60} and FULP in solution. This can be seen by looking a T_{NL}, but especially to the attenuation factor, which is the ratio of T_{lin} over T_{NL}. Notice that all the reported NL transmission data have been measured for input energies well below the damage threshold (~15 J/cm^2 for this sample at 690 nm) and with a not too tightly focused laser beam propagating into 10 mm path length liquid cells. As a result, the corresponding laser fluences are well below the values required to reach full saturation of the strongly absorbing triplet level. The differences in input energies and estimated beam waist diameter should be taken into consideration when comparing the attenuation factors of different substances and at different wavelengths. For instance, the larger beam waist at 690 nm partially spoils the enhancement of the OL efficiency in the red region in the case of C_{60}.

Regarding the comparison with FULP at 690 nm, notice that attenuation factor larger than those of C_{60} at the same

Table 1
C_{60} and FULP solutions attenuation factor at 532 nm and 690 nm

T_{lin}	T_{NL}	Attenuation factor	Input energy [mJ]	Beam-waist (∅) [μm]	Fluence [J/cm^2]
C_{60}@532 nm					
0.77	0.30	**2.6**	0.32	70	2.08
0.66	0.175	**3.8**	0.63	80–90	2.78
0.62	0.15	**4.0**	0.56	80–90	2.47
C_{60}@690 nm					
0.87	0.15	**5.8**	1.00	200	0.80
FULP@532 nm					
0.78	0.27	**3.0**	0.40	200	0.32
0.74	0.25	**3.1**	0.63	200	0.50
0.74	0.15	**5.0**	0.40	100	1.27
FULP@690 nm					
0.92	0.20	**4.6**	0.56	>200	<0.45
0.74	0.10	**7.4**	0.32	>200	<0.25
0.74	0.05	**14.8**	0.32	200	0.25
0.40	0.025	**16.0**	0.79	>200	<0.63

Table 2
FULP sol–gel samples attenuation factor at 690 nm

Thickness [mm]	Concentration [M] [M]	T_{lin}	T_{NL}	Attenuation factor	Input energy [mJ]	Beam waist (Ø) [μm]	Fluence [J/cm^2]
2-layer sample, 100 μm doped, 2150 μm total thickness							
0.1	$2.0\cdot10^{-3}$	0.90	0.17	**7.0**	1.0	100–200	1.42
4-layer sample, 200 μm doped, 2150 μm total thickness							
0.2	$9.7\cdot10^{-4}$	0.90	0.20	**4.5**	1.0	>200	<0.80
6-layer sample, 600 μm doped, 2150 μm total thickness							
0.6	$3.9\cdot10^{-4}$	0.90	0.27	**3.3**	1.0	>200	<0.80
10-layer sample, 500 μm doped, 2150 μm total thickness							
0.5	$8.1\cdot10^{-3}$	0.77	0.10	**7.7**	0.70	200	0.56
Bulk sample							
0.6	$7.4\cdot10^{-3}$	0.63	0.025	**25**	0.56	~100	~1.78

wavelength are obtained for lower input energy and comparable or larger beam waist.

The OL data of sol gel samples collected in Table 2 confirm that the limiting properties of FULP are substantially maintained upon inclusion in the solid matrix. The first three samples reported in Table 2 have been prepared in order to investigate the possible role of the fullerene concentration in sol–gel materials. The linear transmittance of these samples has been kept constant by varying the number of FULP doped layers and their thickness while their concentration was decreased from 2.0×10^{-3} M to 3.2×10^{-4} M, that is almost one order of magnitude. The absence of cluster formation was checked for the more concentrated sample by recording their linear absorption spectra. Also, the total number of layers, doped and undoped, was kept constant in order to have the same number of interfaces with sodalime glass layers. In all samples the total thickness was 2.15 mm. It appears that samples with a higher FULP concentration in the active layers exhibit improved OL efficiency. A similar tendency has been reported also for solution samples [17]. This phenomenon and its microscopic origin deserve further investigation. Table 2 also reports data for a bulk sample, 0.62 mm thick, containing FULP at a concentration of 7.43×10^{-3} M. A value of attenuation factor = 25 was obtained for this sample, showing that high performance OL materials can indeed be obtained with our sol–gel samples. By observing the experimental values of FULP solutions and sol–gel sample it is possible to see that in a non optimized configuration we reach good attenuation factors, with solutions and sol–gel samples, having appropriate linear transmittance.

The use of our sol–gel matrices, allows us to obtain samples with good linear and NL optical properties and small scattering effects. This is very important for the design and preparation of a protection device for real uses, like the ''bottleneck'' [9] device: a multilayer structure with controlled thickness of the layers and concentration of the active molecules.

In the bottleneck device the architecture is based on a set of absorbing layers interleaved with non absorbing ones. The thickness and location of the layers and the concentration of the active molecules are chosen, for a given focusing optics, for optimizing the OL response of the system. This is achieved by imposing that, within the active absorbing layers the fluence is always large enough to efficiently populate the triplet state, but no larger than the damage threshold of our matrix. The ideal optical limiter must have a 10^4 attenuation factor and high linear transmittance (approx. 70%). For the bottleneck architecture we have chosen an $f/5$ focusing optics, obtained by using a short focal lens (50 mm), with an input beam size of ~10 mm. Such a fast focusing optics is needed so that the decreasing of fluence due to the sample absorption is balanced by the decrease of beam size; in such way, a large enough fluence is present within the whole sample.

The positioning of the layers with respect to the focus and the knowledge of the beam sizes within the samples are very critical points for obtaining a good performance from the device. For these reasons we have used Z-scan measurements to investigate, the best position of the samples within our fast focusing system.

The Z-scan and OL curves of our three-layer test sample, with 84% linear transmittance, $8\cdot10^{-3}$ M FULP concentration of the active layers and 1 mm total thickness are reported in Fig. 4. The OL measurements were made in two different positions: in the minimum of the Z-scan curve and 1.5 mm backward. The measurements show that there is a critical dependence on the positioning of the samples. The best response of our test sample shows, however, that the measured attenuation factor (~10) fall short of the calculated one (250). This discrepancy can be understood by different considerations. The calculation for positioning the layers, obtained according to Miles [9],

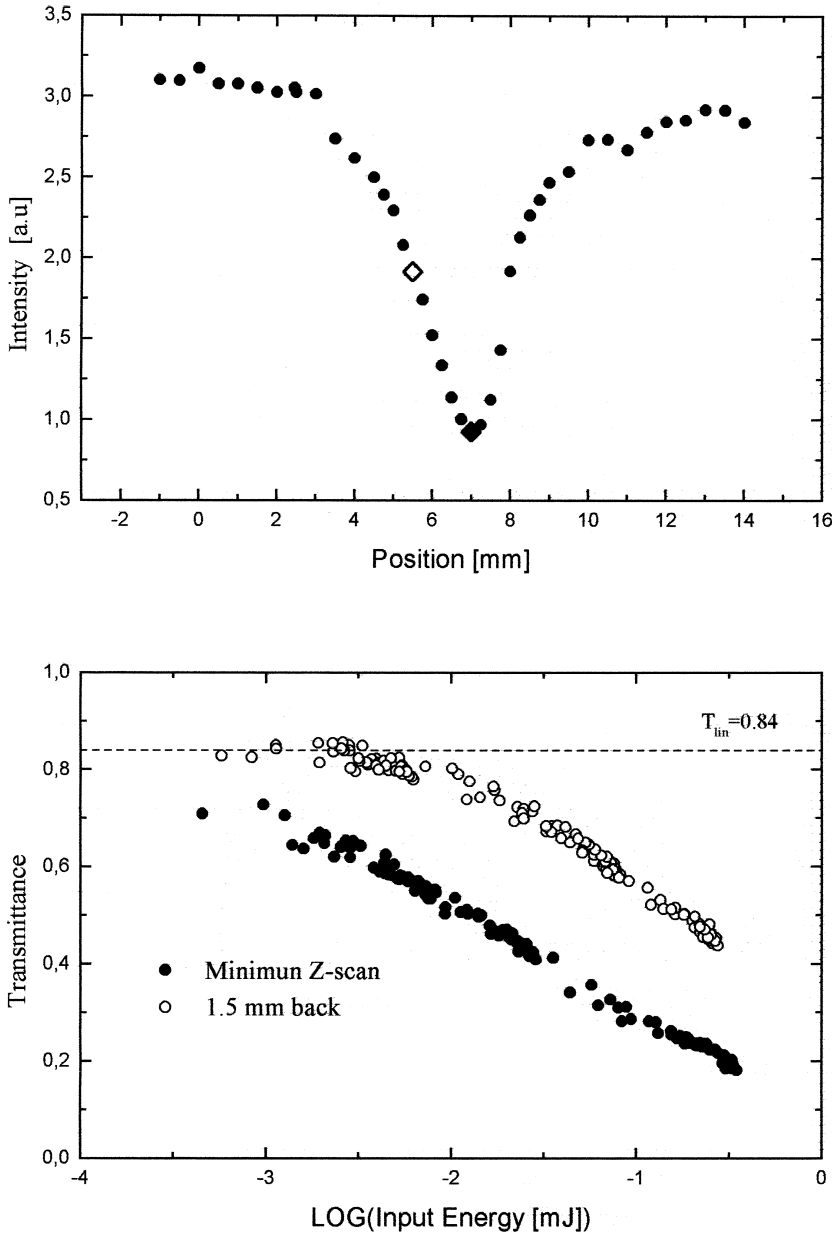

Fig. 4. Open aperture Z-scan (upper panel) and OL (lower panel) data of a three layers bottleneck structure composed of sol–gel films containing FULP measured at 690 nm, with $f/5$ focusing optics. Open and closed circles, in the OL data, are used for data with different position with respect to the focus: open circle in the maximum of absorption, closed 1.5 mm backward.

were made by using a propagation geometry, which is simplified in that diffraction effects are neglected. This would only apply for distances of several Rayleigh ranges from the focal plane. The non linear propagation properties can strongly modify the beam propagation geometry and the intensity distribution can be different from the top-hat intensity distribution used for the calculation. In these cases the real fluence within the sample is less than the calculated one and the device does not work at its maximum efficiency. A better consideration of the real beam propagation is under development.

In order to understand the microscopic mechanism of OL in our samples and estimate the RSA contribution, it is convenient to compare the experimental results with OL curves calculated using an RSA model. To describe the dynamics of the population of the levels shown in Fig. 1, one can use kinetic equations [15,16,18,19], where all possible transitions due to one-photon absorption as well

as all excited state relaxation processes are considered. The total absorption of the system is a function of the sample concentration and thickness and of an effective absorption cross section. The latter quantity is a weighted average of the cross sections of the ground and excited singlet and triplet states. The weights are the fractional populations of these states which, in turn, are a function of the energy, spatial and temporal shape of the input pulse and of the position of the active molecules along the beam path.

For thick samples the calculation is carried out as follows. The input beam is assumed to have a Gaussian temporal profile and a top-hat spatial intensity distribution. To take into account the convergence of the beam, the sample is divided into 10 slices. The program solves the coupled rate equations and gives the change of population distribution in the electronic levels as a function of the fluence of the input beam. The transmission properties are then calculated from the propagation equation.

To fit our experimental OL data for fullerene and FULP solutions, at different wavelengths, it is necessary to know the related photophysical parameters. For this reason we chose a consistent set of parameters, σ_g^S from linear absorption spectra and σ_e^T and τ_i from literature data [2,3,6–8]. The values of these were used as starting point although only minor variations were needed for a fitting of the experimental data. By comparing experimental and calculated OL curves (full lines in Fig. 5) one sees that our RSA model fits well the OL data for low input energies. At high energies the observed discrepancies suggest that other NL effects, like NL scattering, thermal lensing and two-photon absorption (TPA) may play a role.

To investigate these possible concurrent phenomena, we have done OL measurements with open and closed aperture. This makes it possible to investigate non linear scattering phenomena. The collecting angle with the open aperture configuration is 0.475 sterad and with the closed aperture configuration is $3.88 \cdot 10^{-4}$ sterad. It turns out that the collecting angle of our closed aperture configuration is large enough to collect the entire output beam, independent of any refracting effects. Thus, by comparing open and closed aperture OL made with these collecting angles we investigate only NL scattering effects.

OL measurements of C_{60} solution at 532 nm (upper panel) and 690 nm (lower panel), are reported in Fig. 6. Solutions of C_{60} are measured in the open (circles) and closed (triangles) aperture configurations. One sees that, especially for C_{60} solution at 532 nm, there is a large difference between open and closed aperture measurements, namely the contribution of the NL scattering to the total OL is significant [24].

For FULP solution, reported in Fig. 7, and FULP doped sol–gel samples, one can see that the scattering contribution is less significant, both in the green and the red regions. This suggests that the NL scattering gives a large contribution in particular to the OL of C_{60} solution at 532 nm. These measurements show that it is necessary to consider also different NL effects, like thermal lensing and NL absorption.

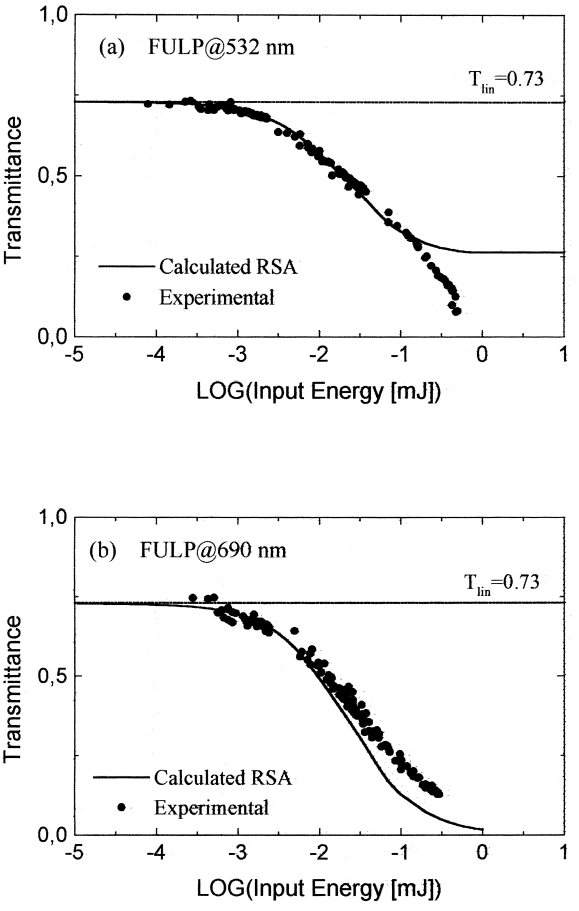

Fig. 5. Experimental (points) and calculated (line) OL data on a FULP solution in toluene at 532 nm (upper panel) and 690 nm (lower panel).

Thermal lensing causes changes of the beam propagation properties within the sample. It has already been demonstrated, by Z-scan measurements [20–23], that C_{60} shows a negative lens effect at 532 nm. By detecting, with an appropriate CCD camera, the beam-waist size during OL measurements it is possible to evaluate the beam variations as a function of the input energies and find out at which input pulse energy the thermal lensing effect starts to be appreciable. Preliminary results [24] confirm the presence of significant thermal lensing effects in solutions and smaller effects in our sol–gel samples.

4. Final remarks

In order to understand the potentiality of pyrrolidinofullerenes it is possible to compare optical properties of FULP at 690 nm with those of Sn-phthalocyanine (Sn-Pc)

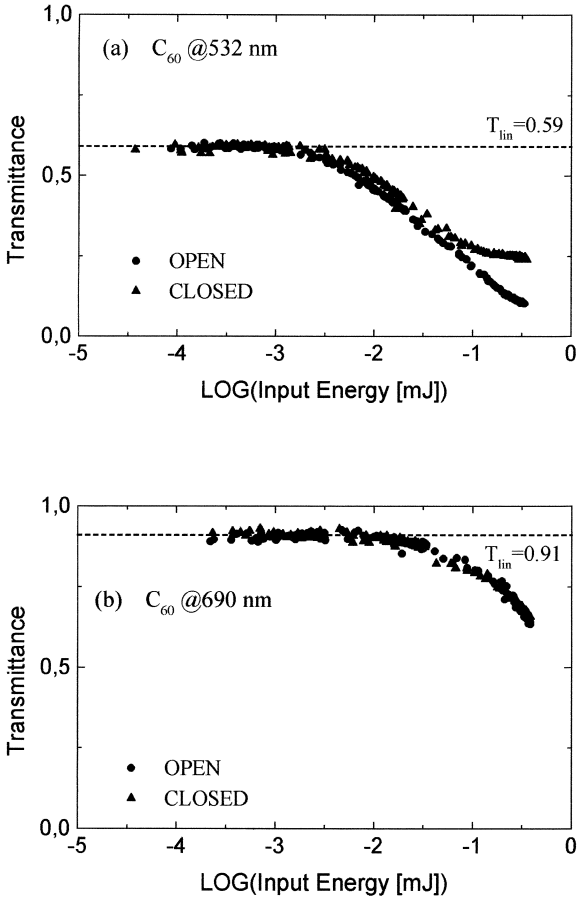

Fig. 6. Open (circles) and closed (triangles) aperture OL measurements of the C_{60} solution in toluene at 532 nm (upper panel) and 690 nm (lower panel).

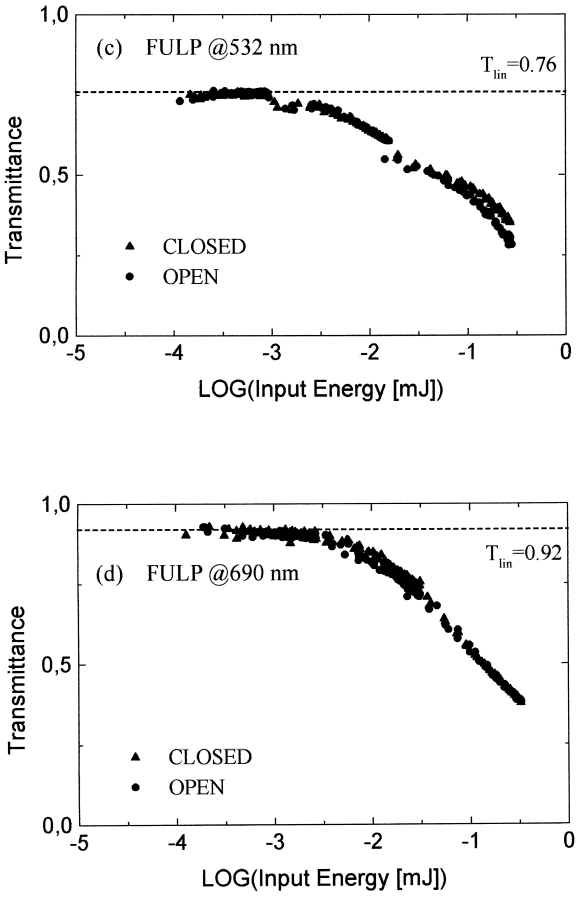

Fig. 7. Open (circles) and closed (triangles) aperture OL measurements of the FULP solution in toluene at 532 nm (upper panel) and 690 nm (lower panel).

[9,25] at 532 nm, which is considered to be one of the best RSA materials in the green region. The comparison is possible by calculating the Fig. of merit (FOM) [26] and the saturation fluence F_S ($F_S = h\nu/\Phi\sigma_g$) of both samples. The calculated data are reported in Table 3. They show that FULP at 690 nm has almost the same performances as Sn-Pc at 532 nm. Therefore, one concludes that materials based on FULP are good RSA materials in the red region. One more parameter has to be considered, however, for characterizing an optical limiter: the 'photopic transmission'. The photopic transmission [27] is defined as the average of the transmission of the protection device in accordance with eye sensitivity:

$$T_{ph} = \frac{\int_{\Delta\lambda} V(\lambda)S(\lambda)T(\lambda)\,d\lambda}{\int_{\Delta\lambda} S(\lambda)V(\lambda)\,d\lambda}$$

$V(\lambda)$ is the ocular relative spectral sensitivity for day vision, $S(\lambda)$ is the spectral distribution of a normalized illuminant and $T(\lambda)$ is the spectral transmission of the protection filter. For eye protection, the photopic transmission is recommended to be greater than 15–20%, since this assures that the protection device does not drastically cut any wavelength in all the visible range. We calculated the photopic transmittance of FULP and Sn-Pc solution having similar T_{lin} respectively in the red and the green region. FULP shows a large photopic transmission with solution having high T_{lin}. It is thus possible to increase the concentration, with an acceptable loss of visibility, and gain room for the transparency/efficiency trade-off typical of RSA-based limiters.

For all these considerations one can conclude that our pyrrolidino-fullerenes are good molecules for OL materials in the red region and can be used, incorporated in a sol–gel matrix, for protection devices.

Table 3
Comparison of FOM's for FULP and Sn-Pc

FULP@690 nm	Sn-Pc @ 532 nm
$\sigma_g = 1.1 \cdot 10^{-18}$ cm^2	$\sigma_g = 2.1 \cdot 10^{-18}$ cm^2
$\sigma_e = 6.2 \cdot 10^{-17}$ cm^2	$\sigma_e = 6.7 \cdot 10^{-17}$ cm^2
(FOM) $\sigma_e - \sigma_g = 6.1 \cdot 10^{-17}$ cm^2	$\sigma_e - \sigma_g = 6.5 \cdot 10^{-17}$ cm^2
$\Phi = 0.85 \div 0.90$	$\Phi = 0.55$
$F_S = 0.31$ J/cm^2	$F_S = 0.33$ J/cm^2
$T_{PH} = 39\%$ ($T_{lin} = 71\%$ at 690 nm)	$T_{PH} = 20\%$ ($T_{lin} = 71\%$ at 532 nm)

Acknowledgements

We thank the European Commission (DG XII) for financial support through contract BRPR-CT97-0564 and CNR L.95/95.

References

[1] Tutt LW, Boggest TF. Prog Quant Electr 1993;17:299–338.
[2] Ebbesen TW, Tanigaki K, Kuroshima S. Chem Phys Lett 1991;181(6):501–4.
[3] Bensasson RV, Hill T, Lambert C, Land EJ, Leach S, Truscott TG. Chem Phys Lett 1993;201(1–4):326–35.
[4] Kost A et al. Opt Lett 1993;18(5):334–6.
[5] Maggini M et al. Adv Mat 1995;7(4):404–6.
[6] Anderson JL, An Y-Z, Rubin Y, Foot CS. J Am Chem Soc 1994;116:9763–4.
[7] Bensasson RV, Bienvenue E, Janot J-M, Leach S, Seta P, Schuster DI, Wilson SR, Zhao H. Chem Phys Lett 1995;245:566.
[8] Williams RM, Zwier JM, Verhoeven JW. J Am Chem Soc 1995;117:4093.
[9] Miles PA. Appl Opt 1994;33:6965–79.
[10] Maggini M, Scorrano G, Prato M. J Am Chem Soc 1993;115:9798–9.
[11] Bianco A et al. J Am Chem Soc 1997;119:7550–4.
[12] Maggini M et al. Chem Eur J 1999;5(9):2501–10.
[13] Brusatin G et al. SPIE proceedings 1999:in press.
[14] Sheik-Bahae M, Said AA, Wei TH, Van Stryland EW. IEEE J Quantum Electron 1990;26:760.
[15] Signorini R et al. NLO section B 1999;21(1–4):143–62.
[16] Signorini R et al. NATO ASI series 1999:in press.
[17] Riggs et al. J Phys Chem 1999;103:485.
[18] Henari F et al. Chem Phys Lett 1992;199(1–2):144–8.
[19] Li C et al. Opt Soc Am B 1994;11(8):1356–60.
[20] Mishra SR et al. J Phys B, At Mol Opt Phys 1994;27:L157–63.
[21] Mishra SR, Rawat HS, Joshi MP, Mehendale SC. Appl Phys A 1996;63:223–6.
[22] Justus BL, Kafafi ZH, Huston AL. Opt Lett 1993;18(19):1603–5.
[23] Rao SV et al. Chem Phys Lett 1998;297:491–8.
[24] Signorini R et al., to be published.
[25] Perry JW et al. Opt Lett 1994;19(9):625–7.
[26] Hagan DJ et al. Mat Res Soc Symp Proc 1995;347.
[27] Lauth H et al., personal communication.